Relocation of the 2011 off the Pacific coast of Tohoku earthquake sequence and fault planes of $M \geq 7$ earthquakes

Nobuo Hurukawa

Building Research Institute, Tsukuba, Ibaraki 305-0802, Japan

(Received April 7, 2011; Revised May 19, 2011; Accepted May 20, 2011; Online published September 27, 2011)

We relocated foreshocks, mainshock, and aftershocks of the 2011 off the Pacific coast of Tohoku Earthquake (M_w 9.1) using the modified joint hypocenter determination (MJHD) method in order to obtain their precise hypocenters and to identify fault planes of larger earthquakes. We used P-wave arrival times at stations worldwide reported by the U.S. Geological Survey (USGS). We confirmed by relocated hypocenters that the mainshock and aftershocks had occurred along the plate boundary between the North American and Pacific plates. We also confirmed that the M_w 7.5 foreshock, which occurred two days before the mainshock, and the largest aftershock (M_w 7.9), which occurred half an hour after the mainshock, were thrust earthquakes along the plate boundary. The second largest aftershock (M_w 7.6), which was a normal-faulting earthquake and was a bending-stress intraplate event caused by the strain reduction on the subduction thrust, occurred at the outer rise of the Japan Trench and was well relocated with its aftershocks. We found that its fault plane dipped westward and it bounded the aftershock distribution on the seaward side. This implies that the western side of the fault plane had subsided, corresponding with the westward plate subduction.

Key words: 2011 off the Pacific coast of Tohoku Earthquake, relocation, fault plane, joint hypocenter determination.

1. Introduction

An M_w 9.1 earthquake occurred off the Pacific coast of Tohoku on March 11, 2011 and caused severe damage in the Tohoku and Kanto districts of the northeastern part of Japan. This was a thrust earthquake occurring at the boundary between the North American and Pacific plates. An M_w 7.5 foreshock preceded the mainshock on March 9 and many large aftershocks including, two M_w 7-class aftershocks, followed the mainshock. Although the mainshock was a thrust earthquake as indicated in global centroid moment tensor (CMT) solutions as produced by Dziewonski *et al*. (1981) and later updates, preliminary hypocenters estimated by the U.S. Geological Survey (USGS) did not correspond well with the plate boundary thrust. This is to be expected if the depths determined by the USGS were not well resolved. Furthermore, it was quite difficult to identify the fault plane for the second M_w 7 aftershock, the mechanism of which was normal-faulting occurring at the outer rise of the Japan Trench.

An accurate and detailed hypocenter distribution map is important basic seismological information for understanding the nature of earthquakes, establishing, for example, the area of the mainshock rupture by estimating the extent of aftershocks in the first day. Therefore, using global phase data reported by the USGS and openly available from their website, we relocated the off the Pacific coast of Tohoku mainshock of March 11, 2011, and its foreshocks and aftershocks. We then identified the preferred fault planes of the $M \geq 7$ earthquakes in the sequence, from the candidate fault planes provided by the global CMT solutions.

2. Method

To precisely relocate hypocenters, we employed the modified joint hypocenter determination (MJHD) method developed by Hurukawa and Imoto (1990, 1992). Because of the lateral heterogeneity of the Earth, the assumption of the horizontally homogeneous velocity model, as normally used in standard hypocenter determination, is inadequate to obtain the precise location of earthquakes. The joint hypocenter determination (JHD) method (Douglas, 1967; Freedman, 1967) enables us to simultaneously relocate many earthquakes, thereby removing the effects of lateral heterogeneity within the Earth. Therefore, we define a station correction that accounts for lateral heterogeneity in the Earth. JHD solutions may, however, become unstable and unreliable as a result of the trade-off between station corrections and estimated focal depths, given the heterogeneous nature of the Earth's structure and in cases of poor station coverage. For this reason, Hurukawa and Imoto (1990, 1992) developed the MJHD method for locating local earthquakes, in which station correction is independent of both the distance and azimuth from the center of the studied region to the given station, thereby improving the stability of the method. Subsequently, Hurukawa (1995) extended the MJHD method for locating teleseismic earthquakes; we use this extended version in this study, and we used the iasp91 model for the estimation of travel times.

Copyright © The Society of Geomagnetism and Earth, Planetary and Space Sciences (SGEPSS); The Seismological Society of Japan; The Volcanological Society of Japan; The Geodetic Society of Japan; The Japanese Society for Planetary Sciences; TERRAPUB.

doi:10.5047/eps.2011.05.027

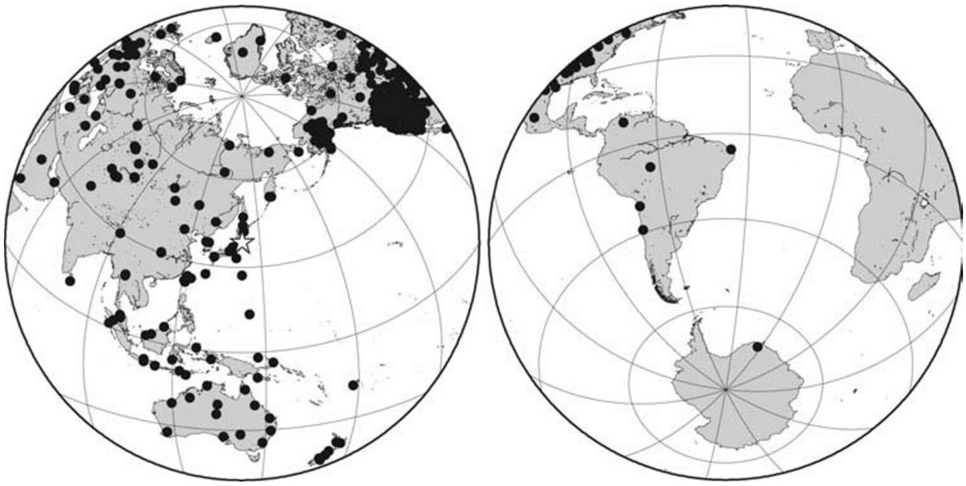

Fig. 1. Distribution of stations used for relocations. The star indicates the epicenter of the mainshock.

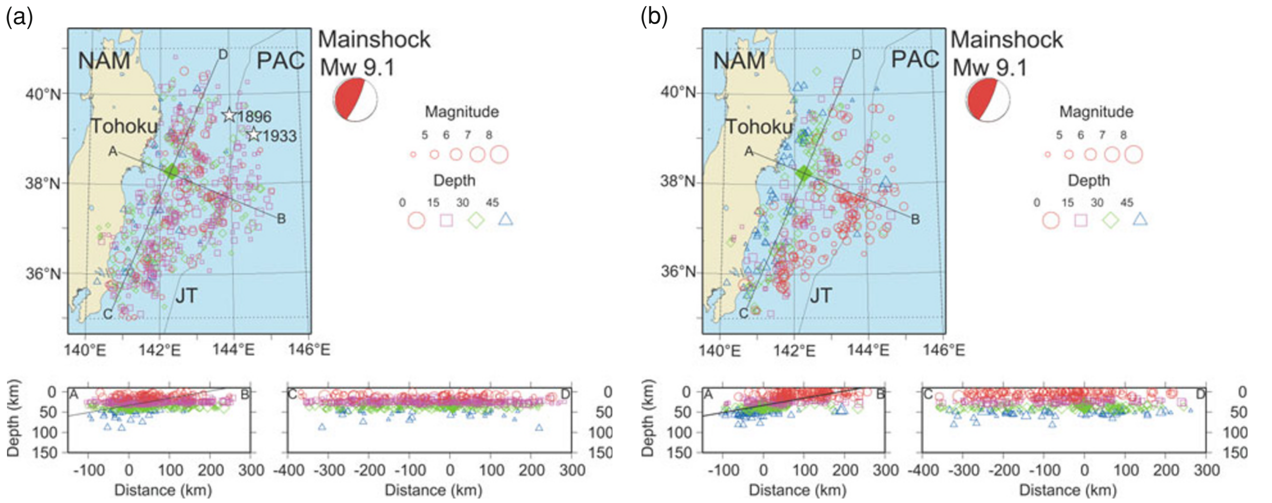

Fig. 2. Epicentral distribution and depth cross-sections along A–B and C–D. A solid symbol indicates the mainshock. The global CMT solution of the mainshock (Dziewonski *et al*. (1981) and later updates) is also shown. Strike A–B is perpendicular to the strike of the WNW-dipping nodal plane of the global CMT solution. (a) USGS locations. Two stars indicate epicenters of the historical 1896 (M 8.2) and 1933 (M_w 8.4) Sanriku earthquakes. (b) Relocated hypocenters by the MJHD method in this study. NAM: North American plate. PAC: Pacific plate. JT: Japan Trench.

3. Data

We downloaded the mchedrqed.dat file of hypocenters and phase arrival data for the period from 1 to 31 March 2011 from the USGS website. We selected events at all depths within the region with bounds 35.0°N and 41.0°N in latitude and 140.0°E and 146.0°E in longitude. We have used here only first P-wave arrival times, because these are more reliably observed than later S-wave arrival times, and very few S-wave arrivals had been reported at the time. Since the aftershock region is broad, ray paths to each station from the events may be significantly different, in breach of the assumptions made for the method. This may mean that the relative location errors, especially those for focal depth, are poorly estimated. However, our main objective here is to establish the main features of hypocenter distribution, including focal depths, in the source region for this M 9-class earthquake. Thus, in analyzing this vast source region as a single set of events, we have sacrificed some of the precision normally expected in the study of a more compact region.

To calculate MJHD hypocenters, two parameters must be defined: the minimum number of stations (MSTN) that observed each earthquake and the minimum number of events (MEVN) observed at each station. Here, MSTN and MEVN were set to 60 and 60, respectively. During the relocation process, we isolated readings with arrival-time residuals exceeding 2 s and these observations were excluded from later stages. In this process, the number of events observed at some stations became less than 60, so we reset MEVN to 50 for the final hypocenter calculations.

4. Results

We located 459 earthquakes using the 363 stations indicated in Fig. 1. Since nearer stations contribute better to the estimation of focal depths, we selected only earthquakes that were located using at least two stations within 10° epicentral distance. Furthermore, only earthquakes with more precise hypocenters are shown in the following figures, those for which the standard errors of latitude, longitude and focal depth are less than 0.1°, 0.1° and 10 km,

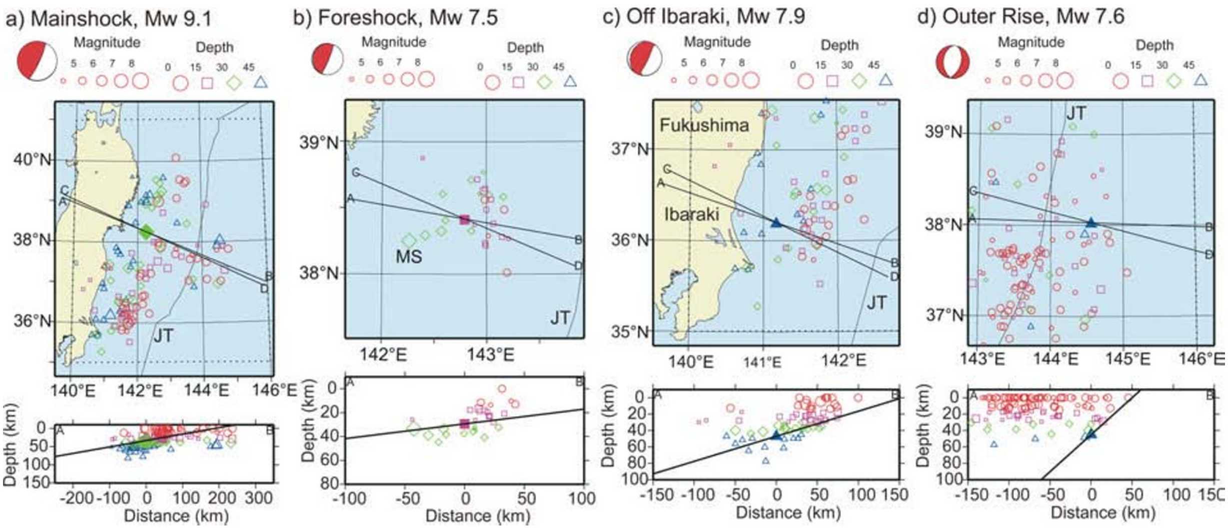

Fig. 3. Relocated hypocenters by the MJHD method in this study. Epicentral distribution and a vertical cross section along the A–B line, which is perpendicular to the strike of the nodal plane of the global CMT solution (Dziewonski *et al*. (1981) and later updates), are shown. This nodal plane corresponds with the fault plane. A C–D line is perpendicular to the strike of the other nodal plane of the global CMT solution. (a) The mainshock (2011/03/11 5:46) and immediate aftershocks within 24 hours. (b) The largest foreshock (2011/03/09 2:45) and its aftershocks. MS indicate the mainshock. (c) The largest M_w 7.9 aftershock off Ibaraki (2011/03/11 6:15) and aftershocks within 24 hours after the mainshock. (d) The M_w 7.6 aftershock at the outer rise (2011/03/11 6:25) and aftershocks.

respectively. The number of earthquakes satisfying these conditions is reduced to 420.

4.1 Mainshock

Figure 2(a) shows the hypocenters of all 619 earthquakes included in the USGS data file, while Fig. 2(b) shows the 420 well-relocated hypocenters determined using the MJHD method in this study. The MJHD hypocenters show a depth dependence across cross-section A–B, which is perpendicular to the nodal axis of the global CMT solution. Relocated focal depths become deeper towards the WNW and correspond with the nodal plane dipping WNW shown projected onto the A–B cross-section. Although the acceptable standard error of focal depth for event solutions was set as less than 10 km, the scatter of computed hypocenters from the mainshock fault plane projection is more than 10 km. The cause of this scattering, if not due to off-fault seismicity, may be partly attributable to lateral heterogeneity in the vicinity of the fault plane and to the areal extent in the MJHD analysis. Since the study region is 500 km $\times$ 700 km, the assumption that a station correction at each station is constant may be invalid because ray paths from hypocenters to each station may be sufficiently different.

Figure 3(a) shows the MJHD hypocenters of the mainshock and immediate aftershocks that occurred within 24 hours after the mainshock. The relocated MJHD hypocenters in Fig. 3(a) confirm that the fault plane of the mainshock corresponds with the nodal plane of the global CMT solution with a strike of 203° and a dip of 10° towards the WNW. The size of the one-day aftershock area is $\sim$450 km $\times$ $\sim$150 km if the outer rise area is excluded. If the outer rise area is included, the size is $\sim$450 km in the northerly direction and $\sim$400 km in the easterly direction.

Some earthquakes east of the Japan Trench were determined deeper than those near the Japan Trench. These earthquakes, including the M_w 7.6 aftershock, will be discussed in Section 4.4.

4.2 Largest foreshock on March 9, 2011

Two days before the mainshock, an M_w 7.5 foreshock occurred near the mainshock. The relocations for the 24 foreshocks are indicated in Fig. 3(b). The fault plane preferred for the M_w 7.5 foreshock is the nodal plane of the global CMT solution with a strike of 190° and a dip of 7° westward as shown projected in Fig. 3(b). The foreshocks were located ENE of the mainshock. The size of the foreshock area is $\sim$50 km $\times$ $\sim$50 km. The mainshock rupture apparently started near the WSW extension of the rupture for the M_w 7.5 foreshock. Close comparison of Figs. 3(a) and 3(b) suggest that no immediate aftershocks occurred in the foreshock area.

4.3 Largest aftershock off Ibaraki

The largest aftershock of M_w 7.9 occurred off Ibaraki 29 minutes after the mainshock (Fig. 3(c)). Although we cannot distinguish between aftershocks of the mainshock and those of the M_w 7.9 aftershock, we can examine whether the largest aftershock could have occurred on an extension of the fault plane of the mainshock. Relocated aftershocks aligned with the nodal plane dipping WNW, shown as a solid line projected on cross-section A–B of Fig. 3(c), rather than the other nodal plane, which projects almost perpendicular to the solid line. This preferred nodal plane is almost parallel to the fault plane of the mainshock, with the aftershocks mainly located on the SWS extension of the mainshock fault plane. Therefore, the preferred fault plane for the largest aftershock in the global CMT solution is the plane with a strike of 199° and a dip of 17°WNW.

Crustal earthquakes near the coasts of Ibaraki and Fukushima are located well above the subduction thrust (distance -50 to -100 km in Fig. 3(c)). These are mostly normal faulting events with EW tensional axes, caused by EW relaxation after the mainshock slip on the subduction thrust.

Other shallower earthquakes occurred above the rupture of the M_w 7.9 aftershock on the eastern trench side, from 141.5°E to 142.0°E. Seismicity near the trench is very low in this region. Further studies are necessary to understand faulting here in the accretionary prism and to evaluate the potential for a tsunami-generating earthquake near the trench.

4.4 Second largest aftershock near the outer rise

Figure 3(d) shows event solutions in the vicinity of the solution for the M_w 7.6 outer rise aftershock, which occurred 39 minutes after the mainshock. The very different normal-faulting mechanism suggests it was a bending-stress intra-plate event caused by strain reduction on the subduction thrust and an increased tendency for Pacific plate subduction to the west after the mainshock rupture. Earthquakes near and west of the Japan Trench were aftershocks occurring on the mainshock thrust as shown in Figs. 2(b) and 3(a), while outer-rise earthquakes east of the Japan Trench distributed along the nodal plane along the A–B cross-section. Therefore, we conclude that the fault plane of this earthquake is the nodal plane of the global CMT solution with a strike of 182° and a dip of 42° westward. Since this large aftershock was the deepest located in this region, it seems the local normal-faulting rupture started here. No earthquakes occurred east of this fault plane. Hence, the western side of the fault plane of the outer rise aftershock subsided beneath the overriding North American plate and the bending stress is probably less significant further eastwards.

5. Discussion

The 2011 off the Pacific coast of Tohoku Earthquake (M_w 9.1) was the largest earthquake ever recorded in Japan. Two magnitude 8 or larger earthquakes occurred during the last two centuries. They were the 1896 (M 8.2) and 1933 (M_w 8.4) Sanriku earthquakes, which had epicenters as shown in Fig. 2(a). The 1896 (M 8.2) earthquake was a thrust and typical tsunami earthquake (Kanamori, 1972) occurring very close to the Japan Trench as shown in Fig. 2(a). Since no aftershocks of the 2011 off the Pacific coast of Tohoku earthquake occurred near the 1896 mainshock location west of the Japan Trench, it seems the rupture plane of the 1896 earthquake may not have been re-ruptured this time. The 1933 Sanriku earthquake was a normal-faulting earthquake in the Pacific plate beneath the Japan Trench (Kanamori, 1971), located north of the M_w 7.6 aftershock of 2011.

Since there is a dense seismic network in Japan, locations and mechanism solutions for large earthquakes in and around Japan should be well determined by the regional network. Earthquakes nearer the Japan Trench and its outer rise may have poorer regional solutions because of restricted azimuthal coverage and fewer closer stations. This study demonstrates that the global network, whose arrival times are available soon after earthquake occurrences, can be used to locate these earthquakes very precisely. The modified joint hypocenter determination (MJHD) method minimizes the effects of unmodeled lateral inhomogeneities, so that the MJHD hypocenters may serve to identify the fault planes of large earthquakes even in the outer rise regions. For further improvement of locations, it is important to combine both the local data and the global teleseismic data in the MJHD location.

Acknowledgments. We thank anonymous reviewers for their helpful comments. Figures and maps were prepared using Generic Mapping Tools software (Wessel and Smith, 1998).

References

Douglas, A., Joint epicenter determination, *Nature*, **215**, 47–48, 1967.

Dziewonski, A. M., T.-A. Chou, and J. Woodhouse, Determination of earthquake source parameters from waveform data for studies of global and regional seismicity, *J. Geophys. Res.*, **86**, 2825–2852, 1981.

Freedman, H. W., A statistical discussion of P residuals from explosions, Part 2, *Bull. Seismol. Soc. Am.*, **57**, 545–561, 1967.

Hurukawa, N., Quick aftershock relocation of the 1994 Shikotan earthquake and its fault planes, *Geophys. Res. Lett.*, **22**, 3159–3162, 1995.

Hurukawa, N. and M. Imoto, Fine structure of an underground boundary between the Philippine Sea and Pacific plates beneath the Kanto district, Japan, *Zisin (J. Seismol. Soc. Jpn.)*, **43**, 413–429, 1990 (in Japanese with an English abstract).

Hurukawa, N. and M. Imoto, Subducting oceanic crust of the Philippine Sea and Pacific plates and weak-zone-normal compression in Kanto district, Japan, *Geophys. J. Int.*, **109**, 639–652, 1992.

Kanamori, H., Seismological evidence for a lithospheric normal faulting—the Sanriku earthquake of 1933, *Phys. Earth Planet. Inter.*, **4**, 289–300, 1971.

Kanamori, H., Mechanism of tsunami earthquakes, *Phys. Earth Planet. Inter.*, **6**, 346–359, 1972.

Wessel, P. and W. H. F. Smith, New, improved version of the Generic Mapping Tools released, *Eos Trans. AGU*, **79**, 579, 1998.

N. Hurukawa (e-mail: hurukawa@kenken.go.jp)